TET1 controls *Cxcl1* induction by DNA demethylation and promotes neutrophil recruitment during acute lung injury

Kathleen M. Yee[1, 2], Richard W. Shuai[3], Bin Liu[1], Christian A. Huynh[1], Chao Niu[1], Hailey R. Lee[1], Min S. Lee[1], Jirui Wen[4, 5], Jian Zou[4, 6*], Jiang Wu[4*], and Ke Shuai[1,2*]

[1]Division of Hematology-Oncology, Department of Medicine; [2]Department of Biological Chemistry; University of California Los Angeles, Los Angeles, California 90095, U.S.A.
[3]Department of Electrical Engineering and Computer Sciences, University of California Berkeley, Berkeley, California 94720, U.S.A.
[4]Deep Underground Space Medical Center, West China Hospital; [5]West China School of Basic Medical Sciences & Forensic Medicine; [6]Department of Otolaryngology Head & Neck Surgery; Sichuan University, Chengdu, China

*Corresponding authors: Jian Zou: zoujian926@163.com; Jiang Wu: jw@scu.edu.cn; Ke Shuai: kshuai@mednet.ucla.edu

Contact author: Ke Shuai
Division of Hematology/Oncology, 11-934 Factor Bldg.,10833 Le Conte Avenue, Los Angeles, California 90095 Tel: 310-206-9168; Fax: 310-825-2493 Email: kshuai@mednet.ucla.edu

Running Title: TET1 in *Cxcl1* induction and neutrophil recruitment

Text word count: 3996; Abstract word count: 246; Figure count: 6; Table count: 0; Reference count: 64

Key Points

- **TET1 has a striking specificity in macrophage gene regulation and controls *Cxcl1* induction by inflammatory stimuli via DNA demethylation**

- **Neutrophil recruitment is defective in *Tet1* deficient mice during acute lung injury**

Abstract

Neutrophils are rapidly recruited from the peripheral blood to the inflammatory site to initiate inflammatory response against pathogenic infections. The process to recruit neutrophils must be properly regulated since the abnormal accumulation of neutrophils can cause organ damage and dysfunction. The acute respiratory distress syndrome (ARDS)/acute lung injury (ALI) is a common cause of respiratory failure that is characterized by the infiltration of neutrophils and epithelial integrity disruption. Indeed, recent studies suggest a pathogenic role of neutrophils in the clinic severity of the coronavirus disease 2019 (COVID-19) ARDS. The chemokine CXCL1, which is rapidly induced by inflammatory stimuli, plays a key role in neutrophil influx during lung inflammation. The molecular basis of *Cxcl1* induction is not fully understood. Here we report that TET1, a member of the ten eleven translocation (TET) methylcytosine dioxygenase protein family, displays a striking specificity in the regulation of gene expression in macrophages. RNA sequencing (RNA-seq) analysis showed that *Tet1* disruption significantly altered the expression of only 48 genes that include *Cxcl1* and several other genes known to be important for cell migration and trafficking in bone marrow derived macrophages (BMDMs) in response to LPS stimulation. TET1 regulates the induction of *Cxcl1* by facilitating the DNA demethylation of the *Cxcl1* promoter. In *Tet1*$^{-/-}$ mice, the induction of *Cxcl1* was suppressed, resulting in defective neutrophil recruitment to the lung during LPS-induced acute lung injury. Our results identify a novel epigenetic mechanism that selectively controls *Cxcl1* induction and neutrophil recruitment during acute lung injury.

Introduction

The acute respiratory distress syndrome (ARDS)/acute lung injury (ALI) is a common cause of respiratory failure that is associated with a high mortality, which ranges from 30% to 40% [1]. The coronavirus disease 2019 (COVID-19) is caused by severe acute respiratory syndrome coronavirus 2 (SARS-CoV-2), and 10-15% of COVID-19 patients progress to ARDS [2,3]. Neutrophils represent the first line of defense in response to invading pathogens and they are the key effector cells during tissue injury-induced inflammation [4-6]. Upon pathogenic infections, neutrophils are rapidly recruited from the peripheral blood to the inflammatory site where they participate in the eradication of microbial infections. Individuals with a deficiency in neutrophils are more susceptible to infections. However, the process to recruit neutrophils to initiate inflammatory response must be properly regulated as the abnormal accumulation of neutrophils at the inflammatory site can cause organ damage and dysfunction [5,7,8]. The role of neutrophils in ARDS/ALI is highlighted by their increased recruitment in the pulmonary capillary bed and into the alveolar space [9]. Recent studies suggest a pathological role for neutrophils and neutrophil-derived neutrophil extracellular traps (NETs) in the clinic severity of COVID-19 [10-14]. Understanding the mechanisms underlying neutrophil recruitment is important for the development of treatment strategies for ARDS/ALI.

The chemokine CXCL1 signals through its receptor CXCR2 to regulate cell migration and recruitment in immune defense, wound healing and tumorigenesis [15-17]. Previous studies have demonstrated a key role of CXCL1 in neutrophil recruitment during lung inflammation [18-22]. It has been well documented that there exists host difference in response to bacterial or viral infections, but the molecular basis involved remains to be poorly understood. Genetic or epigenetic factors may contribute to the differences in host response toward pathogens. In response to inflammatory stimuli, CXCL1 is strongly induced, and transcription factors NF-κB

and STAT1 are shown to be involved in *Cxcl1* induction [23]. The hypermethylation of *Cxcl1* promoter was observed in certain cancer cells [24]. Whether epigenetic mechanism is involved in the transcriptional regulation of *Cxcl1* during inflammation is not known.

DNA modifications such as 5-hydroxymethylcytosine (5hmC) are catalyzed by the ten eleven translocation (TET) methylcytosine dioxygenase protein family, and TET proteins are known to participate in the DNA demethylation process [25-32]. Gene targeting studies have uncovered a key role of TET proteins in multiple cellular processes [33-38]. The role of TET proteins in immune regulation is best exemplified by the finding that TET2 acts to restrict the production of inflammatory cytokines such as IL-6 and IL-1β in macrophages [38], and the loss of TET2 results in clonal hematopoiesis and accelerates atherosclerosis [39,40]. Surprisingly, despite the well established enzymatic role of TET2 in promoting DNA demethylation, it was found that TET2 functions as a transcriptional repressor to suppress inflammatory gene activation by recruiting histone deacetylases (HDACs), a mechanism that is independent of its activity in DNA demethylation [38,39]. These findings have raised an interesting question on whether the TET-mediated DNA demethylation plays an important role in immune regulation.

In this report, we describe a highly specific role of TET1 in the regulation of *Cxcl1* induction in response to inflammatory stimuli such as LPS and TNFα. TET1 acts by regulating the DNA methylation of the *Cxcl1* promoter. We demonstrated that the TET1-CXCL1 regulatory pathway is important for the recruitment of neutrophils during acute lung injury.

Materials and methods

Animal treatment

The animal work conducted in this manuscript was approved by the Animal Research Committee of the University of California Los Angeles. *Tet1*$^{+/-}$ mice in C57BL/6 129Sv genetic background [41] were purchased from the Jackson lab and have been backcrossed to C57 or 129 background for 10 generations. For acute lung injury experiment, WT and *Tet1*$^{-/-}$ mice were intranasally injected with 0.5mg/kg LPS (E. coli 0111:B4, Sigma) for 4 hr.

Primary cell cultures

Mouse bone marrow-derived macrophages (BMDMs) were prepared as previous described [42]. Briefly, bone marrow was flushed from the lower leg bones of mice and subsequently treated with ACK buffer (0.15 M NH4Cl, 10 mM KHCO3, 0.1 mM EDTA) to lyse red blood cells. Then 3 x10^5 cells were seeded per 35 mm well with media containing DMEM, 10% FBS, 1% penicillin-streptomycin and 30% L929 conditioned media. Media was changed at either day 3 or day 4. At day 7 cells were used for experiments.

For preparing mouse embryonic fibroblast cells (MEF), mouse embryos were collected around embryonic day 14. Briefly, visible organs such as the brain, liver, and spleen were removed, and the leftover tissue was quickly minced and incubated in 0.25% trypsin-EDTA for 2 hr at 37°C. Cells were then washed with media and seeded in DMEM with 10% FBS, 1% penicillin/streptomycin and 0.055 mM β-mercaptoethanol. Every three days cells were passaged. Starting at passage 2, cells were used for experiments.

RNA sequencing and analysis

Bone marrow derived macrophages from WT and *Tet1*$^{-/-}$ mice were untreated or treated with LPS for 4 hr. Total RNA was collected and prepared with STAT60 (Tel-Test, Inc.) according to manufacturer's protocol, and was then column purified using RNA Clean and Concentrator (Zymo Research), according to manufacturer's protocol. Library preparation, amplification, and RNA sequencing (HiSeq3000) were performed by the UCLA Technology Center for Genomics and Bioinformatics (TCGB) core.

For RNAseq analysis, the raw sequencing reads (FASTQ files) were first preprocessed to remove low-quality reads and bases. The data was screened for contamination with FASTQScreen, and the quality of the FASTQ sequencing data was assessed with FastQC [43] (http://www.bioinformatics.babraham.ac.uk/projects/fastqc/). Alignment and differential gene expression analysis were performed using a Snakemake workflow [44]. The reads were aligned to the mm10 reference genome from the Ensembl genome database and counted using STAR [45]. Normalization of raw counts and detection of differentially expressed genes (DEGs) were performed with the DEG elimination strategy (DEGES) from the TCC package using the TMM-(edgeR-TMM)$_3$ pipeline followed by DEG identification with edgeR [46,47]. Adjusted p-values were determined using the Benjamini–Hochberg procedure in identification. Heatmaps were generated using the pheatmap R package (https://cran.r-project.org/package=pheatmap). For display on heatmaps, normalized counts were converted to a $\log_2$ scale, and the z-scores were calculated using the means and standard deviations across the samples for each gene.

Promoter Methylation Analysis

Genomic DNA (gDNA) was converted with sodium bisulfite using the EZ Methylation Gold Kit (Zymo Research) according to manufacturers protocol. *Cxcl1* promoter regions #1 and #2 were PCR amplified from sodium bisulfite converted gDNA using ZymoTaq Polymerase (Zymo Research) and purified by gel extraction using the QIAquick Gel Extraction Kit (Qiagen). These

purified PCR products were then cloned into pCR4-TOPO using the TOPO-TA Cloning Kit (Thermo Fisher Scientific) and transformed into chemically competent cells. Minipreps were screened for correctly sized inserts and positive clones were sent for sequencing.

The following primers were used to amplify the *Cxcl1* promoter region from converted gDNA:

Cxcl1 region 1 methylation-5': GGGGTAAAAAGTAAAAATTTTAGAGTTTAAT

Cxcl1 region 1 methylation-3': TCCCAACCATAATCTACAAACACTAACAAC

Cxcl1 region 2 methylation-5': AGTAGGGTAGGGATGTTTTAGGAATTAT

Cxcl1 region 2 methylation-3': TTAAACTCTAAAATTTTTACTTTTTACCCC

Luciferase Reporter Analysis

Cxcl1 promoter region from nucleotide -157 to +283 was cloned into pGL3-basic (Promega) through KpnI and BglII cloning sites using the following primers:

*Cxcl1*_promoter 5': CGGTACCCAAAAAGCAAAAATCCCAGAGT

*Cxcl1*_promoter 3': CAGAGATCTCTCTGGATGTTCTTGAGGTGAA

To create artificially methylated *Cxcl1* promoter in pGL3 expression vector, the PCR-amplified *Cxcl1* promoter fragment was digested with KpnI and BglII (New England Biolabs) and then purified by gel extraction using the QIAquick Gel Extraction Kit (Qiagen). The purified *Cxcl1* promoter fragment was equally split into two groups: one treated with M.SssI (New England Biolabs) and the other without M.SssI ("mock") according to manufacturers' protocol. The two treatment groups were then column purified and ligated into pGL3 basic using T4 ligase (Thermo Fisher Scientific). Luciferase promoter activity was determined using the Dual-Luciferase Reporter Assay System (Promega) according to manufacturer's protocol. 293T cells were transfected by calcium phosphate method with the various pGL3 expression vectors along

with an equal amount of Renilla plasmid. The next day, cells were treated with or without TNF (20 ng/ml) for 5 h to induce *Cxcl1* expression. Firefly luciferase values were normalized by Renilla luciferase expression.

Flow Cytometry Analysis

To collect bronchoalveolar lavage (BAL) fluids, mouse ribs were carefully removed to expose the lung cavity and neck tissues removed to expose the trachea of euthanized mice. A 22 G catheter was then inserted into the trachea. Using a 1 ml syringe, 0.75 ml of cold PBS was injected into the lungs via the catheter and the fluid aspirated out and collected. This was repeated four more times, for a total volume of roughly 3.5 ml. Single cell suspensions of the BAL fluids were stained with various combinations of surface markers followed by flow cytometry analysis using a FACSCalibur or FACScanX (Becton Dickinson, BD). Data were analyzed using the FlowJo software. Neutrophils, macrophages, and eosinophils were identified on the Flow as previously described [48,49]. Specifically, neutrophils were gated as $CD45^{+}CD11b^{+}Ly6G^{+}$ cells, macrophages were identified as $CD45^{+}CD11c^{+}SiglecF^{+}$ population of cells, and eosinophils were defined as $CD45^{+}CD11c^{low/-}SiglecF^{+}$ cells.

Quantitative real time polymerase chain reaction (Q-PCR) analysis

Quantitative real time polymerase chain reaction (Q-PCR) analyses were performed as described [42]. Briefly, cDNA prepared using the iScript cDNA Synthesis kit (Bio-Rad) were analyzed by Q-PCR using the CFX-96 Real-Time Detection System (Bio-Rad). See Supplementary Information for primer sequences of genes analyzed by Q-PCR.

ELISA assays

Enzyme-linked immunosorbent assay (ELISA) kits for CXCL1 (Peprotech) and TNFα (R&D) were used to measure CXCL1 and TNFα protein levels in BAL fluid following the manufacturer's instructions.

Results

Systematic analysis of the role of TET1 in LPS-triggered gene induction by RNA-seq

To examine if TET1 is regulated by inflammatory stimuli, WT and *Tet1*$^{-/-}$ BMDMs were treated with a variety of Toll-like receptor (TLR) ligands followed by Q-PCR analysis. LPS stimulation strongly increased *Tet1* mRNA in WT but not *Tet1*$^{-/-}$ BMDMs. *Tet1* was also induced in response to TLR2 ligand Zymosan and TLR3 agonist Poly(I:C), but not IFNγ or IL-4 (Fig. 1A). These results suggest that TET1 may play a role in TLR signaling.

To examine the role of TET1 in the LPS-induced gene regulation, we performed a non-biased systematic study of gene profiling of WT and *Tet1*$^{-/-}$ BMDMs untreated or treated with LPS for 4 hr by RNA-seq analysis. Surprisingly, as shown in Fig. 1B & 1C, the expression of only a very limited number of genes was significantly affected by *Tet1* deletion either constitutively or upon LPS stimulation (fold change >1.5, adjusted P value <0.05). *Tet1* deletion caused the significant suppression of 32 and 33 genes in untreated or LPS treated cells, respectively, while the removal of TET1 induced only 9 genes in untreated cells and 15 genes upon LPS stimulation.

The most significantly repressed gene caused by *Tet1* deletion upon LPS stimulation is *Cxcl1*, a chemokine known to regulate cell migration and recruitment [15-17] (Fig. 1C). In addition to *Cxcl1*, *Tet1* disruption also resulted in the altered expression of a number of genes known to regulate cell migration and trafficking under various physiological settings, including chondroitin sulfate proteoglycan 4 (*Cspg4*), cytoplasmic polyadenylation element-binding protein 1 (*Cpeb1*), serine protease HTRA4 (*Htra4*), proteoglycan 4 (*Prg4*), and N-acetyllactosaminide beta-1,3-N-acetylglucosaminyltransferase 3 (*B3gnt3*) [50-55]. Thus, RNA-seq analysis revealed that TET1 displayed a striking specificity in gene regulation with the most recognizable preference for the regulation of genes involved in cell migration and trafficking.

TET1 specifically regulates the induction of *Cxcl1* in multiple cell types

Next, we performed Q-PCR analysis to validate the findings of the RNA-seq studies. The induction of *Cxcl1* was defective in *Tet1*$^{-/-}$ BMDMs in response to LPS stimulation for 2 hr, 6 hr or 24 hr, while the induction of other chemokine genes such as *Cxcl2* and *Cxcl10* was not affected (Fig. 2A). The removal of one copy of *Tet1* (*Tet1*$^{+/-}$) showed only a modest reduction on *Cxcl1* expression as compared to the WT control, and the level of *Cxcl1* in *Tet1*$^{+/-}$ cells was at least 10xfold higher than that in *Tet1*$^{-/-}$ cells (supplementary Fig. S1).

Previous studies indicate that *Tet2* deletion in BMDMs altered the expression of over 450 genes, and caused the up-regulation of inflammatory genes such as *Il-6* and *Il1-*β[40]. Consistent with the RNA-seq results, the induction of inflammatory cytokines such as *Il-6*, *Il-1*β or *Tnf*α was not significantly altered in *Tet1* deficient BMDMs in response to LPS stimulation for 2 hr or 6 hr. However, a prolonged treatment of *Tet1*$^{-/-}$ BMDMs with LPS for 24 hr caused a modest repression of *Il-6* and *Il-1*β. The deletion of *Tet1* had no significant effect on the expression of *Tet2* or *Tet3* (Fig. 2A). Thus, TET1 and TET2 display opposing effects on inflammatory gene expression.

To further validate the specific effect of TET1 on *Cxcl1* expression, we performed Q-PCR analysis utilizing primary peritoneal macrophages isolated from wild type and *Tet1*$^{-/-}$ mice or bone marrow derived dendritic cells (BMDCs) (Fig. S2). Again, the induction of *Cxcl1* was repressed in these cell types. These results support a key role of *Tet1* in the LPS-induced *Cxcl1* expression.

Cxcl1 is known to be induced by other inflammatory cytokines such as TNFα. To test if the observed *Tet1-Cxcl1* regulation also operates in response to inflammatory stimuli other than LPS, we analyzed the effect of *Tet1* disruption on gene induction in response to TNFα or IFNγ in primary embryonic fibroblasts (MEFs) (Fig. 2B). *Cxcl1* was strongly induced by TNFα in WT but not *Tet1* deficient fibroblasts. Again, the induction of *Cxcl2* was not affected. *Cxcl1* was also induced by IFNγ in wild type MEFs, but not in *Tet1* deficient cells. In contrast, the induction of *Cxcl9* by IFNγ was not affected in the absence of TET1. The IFNγ-induced *Cxcl10* was modestly suppressed in *Tet1*$^{-/-}$ MEFs (Fig. 2B). These results indicate that TET1 regulates the induction of *Cxcl1* in response to multiple inflammatory stimuli.

TET1 regulates the promoter DNA methylation of *Cxcl1*

Results from Fig.1 and Fig. 2 indicate that the effect of TET1 in transcription is gene-specific in response to multiple stimuli. Although transcription factors such as STAT1 and NF-κB are known to be involved in the regulation of the expression of *Cxcl1* [23], it is unlikely that these transcription factors are directly involved in the observed specific regulation of *Cxcl1* induction since many well known targets of STAT1 and NF-κB were not affected in *Tet1* deficient cells. We hypothesized that TET1 might regulate *Cxcl1* expression through an epigenetic mechanism since TET1 is known to promote DNA demethylation.

TET proteins can promote DNA demethylation of CpG sites present in gene promoters. We identified two regions (Region #1 and Region #2, Fig. 3) within the *Cxcl1* promoter that contain potential CpG methylation sites. These two regions also contain potential NF-κB or STAT1 binding sequences (Fig. 3). We performed bisulfite-sequencing analysis and showed that these two regions were indeed enriched in CpG methylation in wild type BMDMs (Fig. 3 and Fig. S3). Interestingly, the extent of CpG methylation in Region #1 was clearly increased in *Tet1*-deficient

BMDMs (Fig. 3). In Region #2, the extent of CpG site methylation was near saturation in wild type cells, and *Tet1* disruption did not show significant effect on DNA methylation in this region (Fig. S3). These results indicate that TET1 participate in the CpG site methylation in the region #1 of the *Cxcl1* gene promoter in BMDMs. Similar results were observed in the bisulfite-sequencing analysis of DNA samples from peritoneal macrophages of WT and *Tet1*$^{-/-}$ mice (Fig.S4).

To test if the TET1-mediated regulation of promoter CpG methylation also occurs in cells other than macrophages, we performed bisulfite-sequencing analysis of region #1 of the *Cxcl1* gene promoter using WT and *Tet1*$^{-/-}$ primary embryonic fibroblasts (MEFs). In untreated wild type MEFs, the CpG site methylation in Region #1 was weak (10% to 30%) and was almost completely removed after TNFα stimulation (Fig. 4). In contrast, the CpG site methylation of Region #1 was found to be near 100% and remained to be very high (70% to 100%) after TNFα treatment in *Tet1*-deficient fibroblasts (Fig. 4). Taken together, our results suggest that TET1 controls the promoter DNA methylation of the *Cxcl1* gene in multiple cell types.

The TET1-mediated regulation of *Cxcl1* promoter methylation is important for the induction of *Cxcl1* gene

Next, we performed experiments to test if the TET1-mediated DNA methylation indeed contributes to the regulation of *Cxcl1* gene induction by luciferase assays. We first cloned a DNA fragment containing the Region#1 of the *Cxcl1* gene promoter into a luciferase reporter plasmid (pGL3-CXCL1). Transient transfection of this reporter plasmid in 293T cells showed a strong induction of luciferase activity in response to TNFα stimulation, indicating that the DNA fragment (-157 to +283) in this reporter plasmid indeed functions as the TNF-responsive promoter of *Cxcl1* gene (Fig. 5A).

To examine the role of CpG methylation in gene activation, the *Cxcl1* promoter fragment (nucleotide -157 to +283) was subjected to treatment with the CpG methyltransferase M.SssI *in vitro* as previously described [56]. The M.SssI treated or mocked treated DNA fragments were then cloned into the pGL3 vector plasmid, followed by transient transfection into 293T cells together with the control Renilla plasmid. Consistent with the results from Fig. 5A, the mocked treated *Cxcl1* promoter plasmid showed strong luciferase reporter activity in response to TNFαstimulation. In contrast, the TNFα-induced reporter activity was significantly blocked in cells transfected with the M.SssI treated *Cxcl1* promoter plasmid (Fig. 5B). These studies suggest that the cytosine methylation in the Region #1-containing *Cxcl1* promoter results in the suppression of its promoter activity in response to TNFα treatment. Taken together, our results show that the TET1-mediated CpG demethylation of the Region #1 in the *Cxcl1* promoter may contribute at least in part to the induction of *Cxcl1* in response to LPS or TNFα stimulation.

Tet1 disruption resulted in defective neutrophil recruitment in the LPS-induced mouse model of acute lung injury

CXCL1 plays an important role in neutrophil recruitment. LPS can trigger acute lung injury with neutrophil emigration that contributes to the initiation of lung inflammation [57-60]. We used the LPS-induced mouse model of acute lung injury to examine the physiological significance of the TET1 in neutrophil recruitment during lung inflammation. WT, *Tet1*$^{+/-}$ and *Tet1*$^{-/-}$ mice were subjected to LPS challenge for 4 hr, and BAL fluid was collected and subjected to flow cytometry analysis. As shown in Fig. 6A, the recruitment of neutrophils was significantly reduced in the lungs of *Tet1*$^{-/-}$ mice. We also observed a modest increase of macrophages in the *Tet1*$^{-/-}$ mice, but the distribution of eosinophils was not affected.

Next, we examined the overall CXCL1 protein levels in the BAL fluid by ELISA assays. Upon LPS stimulation, the total level of CXCL1 protein was significantly repressed in the BAL fluid obtained from *Tet1*$^{-/-}$ mice as compared to that from WT and *Tet1*$^{+/-}$ controls (Fig. 6B), which is consistently with the essential role of TET1 in the regulation of *Cxcl1* induction.

TNFα, a critical mediator of inflammation and tissue damage, is produced mainly by neutrophils and macrophages in response to LPS stimulation [61]. To test if the defective neutrophil recruitment observed in *Tet1*$^{-/-}$ mice affects TNFα production in the BAL fluid, ELISA assays were performed to measure the levels of TNFα protein. As shown in Fig. 6C, the production of TNFα was significantly reduced in the BAL fluid of *Tet1*-deficient mice upon LPS challenge, consistent with the defective neutrophil recruitment in the absence of TET1.

We examined the mRNA levels of *Cxcl1* and *Tnfα* in the total cell population present in the BAL fluid following LPS challenge by Q-PCR analysis. Again, the induction of *Cxcl1* was defective in cells isolated from the *Tet1*$^{-/-}$ BAL fluids (Fig. 6D). *Tet1* disruption did not significantly affect the LPS-induced expression of *Tet2*. Consistent with the reduced percentage of neutrophils present in the total cell population of the BAL fluid of the LPS-treated *Tet1*$^{-/-}$ mice (Fig. 6A), the overall mRNA level of *Tnfα* was also repressed (Fig. 6D). These results support the *in vivo* functional role of TET1 in the specific regulation of the LPS-induced *Cxcl1* expression and neutrophil recruitment during acute lung injury.

Discussion

The chemokine CXCL1 plays an important role in immune response and tumorgenesis. CXCL1 functions as a critical chemoattractant for neutrophils during lung inflammation. In cancer, it has been suggested that CXCL1 mediates tumor cell metastasis [62], and is important for the recruitment of myeloid-derived suppressor cells (MDSCs) into the tumor microenvironment [63]. The promoter DNA methylation of *CXCL1* in human cancer cell lines has been observed [24], but its biological significance in tumorigenesis as well as the molecular basis involved is not clear. SETDB2, a histone lysine methyltransferase, was shown to be induced upon pathogenic infection and suppressed the induction of *Cxcl1* [64]. The role of DNA methylation in the regulation of *Cxcl1* has not been understood. In this report, we provide both genetic and biochemical evidences to show that TET1 acts as a specific epigenetic regulator of *Cxcl1* by promoting the DNA demethylation and thus the transcriptional activation of *Cxcl1* in response to inflammatory stimuli such as LPS and TNFα.

A key functional property of TET proteins is their ability to promote DNA demethylation. The role of TET proteins in immune regulation is best exemplified by the finding that TET2 acts to restrict the production of inflammatory cytokines such as IL-6 and IL-1β in macrophages, and the loss of TET2 results in clonal hematopoiesis and accelerates atherosclerosis. In this case, it is proposed that TET2 functions as a transcriptional repressor to suppress inflammatory gene activation by recruiting HDACs, a mechanism that is independent of its activity in DNA demethylation [38-40]. These findings have raised an interesting question on whether the TET-mediated DNA demethylation plays a role in immune regulation. Our studies described in this paper have demonstrated a clear role of TET1 in mediating the promoter DNA demethylation of *Cxcl1*. In contrast to TET2, which functions as a transcriptional repressor in immune gene

activation, TET1 acts as an important activator in the induction of *Cxcl1* in response to inflammatory stimuli. Thus, TET1 and TET2 have opposing effects on immune gene activation.

There is also a clear difference between TET1 and TET2 in their specificity involved in gene regulation in macrophages. Gene profiling by microarray showed that the expression of about 450 genes was altered by more than a factor of 1.5 when compared WT and Tet2$^{-/-}$ macrophage upon LPS stimulation [40]. In contrast, the expression of only 48 genes was affected in *Tet1* deficient macrophages upon LPS stimulation, with the most significant effect on the induction of *Cxcl1*. Thus, TET1 appears to be more specific in immune gene regulation in macrophages. Interestingly, several other genes such as *Cspg4*, *Cpeb1*, *Htra4*, *Prg4*, and *B3gnt3* [50-55] that are known to play a role in cell migration and trafficking were found to be significantly altered by *Tet1* deletion. These results raise an interesting possibility that TET1 may have a broad role in the control of cell migration. The molecular basis for the observed specificity of TET1 in macrophage gene regulation remains to be unclear. One possibility is the presence of a very low amount of TET1 protein in macrophages. In fact, although we could clearly detect *Tet1* mRNA by Q-PCR analysis (Fig. 1A), we were unable to detect TET1 protein in BMDMs or MEFs with different sources of anti-TET1 antibodies (unpublished observation). Thus, it is likely that the cell-type specificity of an epigenetic regulator such as TET1 can be achieved by modulating its level of protein expression.

Consistent with the well-documented importance of CXCL1 in neutrophil recruitment, we showed that the presence of neutrophils in the BAL fluid was significantly suppressed in *Tet1*$^{-/-}$ mice upon LPS challenge as compared to the WT or *Tet1*$^{+/-}$ control mice. In contrast, the distribution of eosinophils in the BAL fluid was not altered by *Tet1* disruption. Interestingly, we observed a modest increase of macrophages in the *Tet1*$^{-/-}$ BAL fluid. Despite the increased resident macrophages which are known to be the major CXCL1-producing cells in the *Tet1*$^{-/-}$

BAL fluid, the level of CXCL1remained to be suppressed, a phenomenon consistent with the conclusion that macrophages with *Tet1* disruption are defective in producing CXCL1. In conclusion, our studies have identified an epigenetic mechanism that regulates the CXCL1-mediated neutrophil recruitment during lung inflammation.

Acknowledgements

We thank the UCLA flow cytometry core facility and the UCLA Technology Center for Genomics and Bioinformatics (TCGB) core facility for technical support. Supported by funds from the UCLA Division of Hematology-Oncology (K.S.), by grants from the Foundation of Sichuan Provincial Science and Technology Program (#2019YFH0158 and #2019YFH0147 to J.Z.), and by Project for Disciplines of Excellence Award from West China Hospital, Sichuan University (ZYJC18016 to J.Z. and J.W.).

Authorship contributions

J.Z., J.W. and K.S. directed the project and designed experiments. K.S., K.M.Y., J.Z., J.W., and R.W.S. wrote the manuscript. K.M.Y. executed most of the experiments. R.W.S. analyzed and interpreted RNA-seq data and performed statistical analysis. B.L., C.A.H., C.N., H.R.L., M.S.L., and J.W. participated in Q-PCR analysis and animal studies.

Conflict of interest

K.S. and B.L. are board directors of Abiocode, Inc.

References

1. Matthay MA, Zemans RL, Zimmerman GA, et al. Acute respiratory distress syndrome. *Nat Rev Dis Primers*. 2019;5(1):18.

2. Hui DS, E IA, Madani TA, et al. The continuing 2019-nCoV epidemic threat of novel coronaviruses to global health - The latest 2019 novel coronavirus outbreak in Wuhan, China. *Int J Infect Dis*. 2020;91:264-266.

3. Pedersen SF, Ho YC. SARS-CoV-2: a storm is raging. *J Clin Invest*. 2020;130(5):2202-2205.

4. Reutershan J, Ley K. Bench-to-bedside review: acute respiratory distress syndrome - how neutrophils migrate into the lung. *Crit Care*. 2004;8(6):453-461.

5. Kolaczkowska E, Kubes P. Neutrophil recruitment and function in health and inflammation. *Nat Rev Immunol*. 2013;13(3):159-175.

6. Mortaz E, Alipoor SD, Adcock IM, Mumby S, Koenderman L. Update on Neutrophil Function in Severe Inflammation. *Front Immunol*. 2018;9:2171.

7. Grommes J, Soehnlein O. Contribution of neutrophils to acute lung injury. *Mol Med*. 2011;17(3-4):293-307.

8. Castanheira FVS, Kubes P. Neutrophils and NETs in modulating acute and chronic inflammation. *Blood*. 2019;133(20):2178-2185.

9. Caudrillier A, Kessenbrock K, Gilliss BM, et al. Platelets induce neutrophil extracellular traps in transfusion-related acute lung injury. *J Clin Invest*. 2012;122(7):2661-2671.

10. Wang D, Hu B, Hu C, et al. Clinical Characteristics of 138 Hospitalized Patients With 2019 Novel Coronavirus-Infected Pneumonia in Wuhan, China. *JAMA*. 2020.

11. Barnes BJ, Adrover JM, Baxter-Stoltzfus A, et al. Targeting potential drivers of COVID-19: Neutrophil extracellular traps. *J Exp Med*. 2020;217(6).

12. Zuo Y, Yalavarthi S, Shi H, et al. Neutrophil extracellular traps in COVID-19. *JCI Insight*. 2020;5(11).

13. Middleton EA, He XY, Denorme F, et al. Neutrophil Extracellular Traps (NETs) Contribute to Immunothrombosis in COVID-19 Acute Respiratory Distress Syndrome. *Blood*. 2020.

14. Hemmat N, Derakhshani A, Bannazadeh Baghi H, Silvestris N, Baradaran B, De Summa S. Neutrophils, Crucial, or Harmful Immune Cells Involved in Coronavirus Infection: A Bioinformatics Study. *Front Genet*. 2020;11:641.

15. Strieter RM, Keane MP, Burdick MD, Sakkour A, Murray LA, Belperio JA. The role of CXCR2/CXCR2 ligands in acute lung injury. *Curr Drug Targets Inflamm Allergy*. 2005;4(3):299-303.

16. Bhatia M, Zemans RL, Jeyaseelan S. Role of chemokines in the pathogenesis of acute lung injury. *Am J Respir Cell Mol Biol*. 2012;46(5):566-572.

17. Gillitzer R, Goebeler M. Chemokines in cutaneous wound healing. *J Leukoc Biol*. 2001;69(4):513-521.

18. Lin M, Carlson E, Diaconu E, Pearlman E. CXCL1/KC and CXCL5/LIX are selectively produced by corneal fibroblasts and mediate neutrophil infiltration to the corneal stroma in LPS keratitis. *J Leukoc Biol*. 2007;81(3):786-792.

19. De Filippo K, Dudeck A, Hasenberg M, et al. Mast cell and macrophage chemokines CXCL1/CXCL2 control the early stage of neutrophil recruitment during tissue inflammation. *Blood*. 2013;121(24):4930-4937.

20. Paudel S, Baral P, Ghimire L, et al. CXCL1 regulates neutrophil homeostasis in pneumonia-derived sepsis caused by Streptococcus pneumoniae serotype 3. *Blood*. 2019;133(12):1335-1345.

21. Jin L, Batra S, Douda DN, Palaniyar N, Jeyaseelan S. CXCL1 contributes to host defense in polymicrobial sepsis via modulating T cell and neutrophil functions. *J Immunol*. 2014;193(7):3549-3558.

22. Sawant KV, Xu R, Cox R, et al. Chemokine CXCL1-Mediated Neutrophil Trafficking in the Lung: Role of CXCR2 Activation. *J Innate Immun*. 2015;7(6):647-658.

23. Burke SJ, Lu D, Sparer TE, et al. NF-kappaB and STAT1 control CXCL1 and CXCL2 gene transcription. *Am J Physiol Endocrinol Metab*. 2014;306(2):E131-149.

24. Zhou C, Chen J, Tang X, et al. DNA methylation and gene expression of the chemokine (C-X-C motif) ligand 1 in patients with deficit and non-deficit schizophrenia. *Psychiatry Res*. 2018;268:82-86.

25. Huang Y, Rao A. Connections between TET proteins and aberrant DNA modification in cancer. *Trends Genet*. 2014;30(10):464-474.

26. Ko M, An J, Pastor WA, Koralov SB, Rajewsky K, Rao A. TET proteins and 5-methylcytosine oxidation in hematological cancers. *Immunol Rev*. 2015;263(1):6-21.

27. Tsagaratou A, Rao A. TET proteins and 5-methylcytosine oxidation in the immune system. *Cold Spring Harb Symp Quant Biol*. 2013;78:1-10.

28. Wu H, Zhang Y. Mechanisms and functions of Tet protein-mediated 5-methylcytosine oxidation. *Genes Dev*. 2011;25(23):2436-2452.

29. Cimmino L, Abdel-Wahab O, Levine RL, Aifantis I. TET family proteins and their role in stem cell differentiation and transformation. *Cell Stem Cell*. 2011;9(3):193-204.

30. Williams K, Christensen J, Helin K. DNA methylation: TET proteins-guardians of CpG islands? *EMBO Rep*. 2012;13(1):28-35.

31. Branco MR, Ficz G, Reik W. Uncovering the role of 5-hydroxymethylcytosine in the epigenome. *Nat Rev Genet*. 2012;13(1):7-13.

32. Guo JU, Su Y, Zhong C, Ming GL, Song H. Emerging roles of TET proteins and 5-hydroxymethylcytosines in active DNA demethylation and beyond. *Cell Cycle*. 2011;10(16):2662-2668.

33. Blaschke K, Ebata KT, Karimi MM, et al. Vitamin C induces Tet-dependent DNA demethylation and a blastocyst-like state in ES cells. *Nature*. 2013;500(7461):222-226.

34. Yamaguchi S, Hong K, Liu R, et al. Tet1 controls meiosis by regulating meiotic gene expression. *Nature*. 2012.

35. Doege CA, Inoue K, Yamashita T, et al. Early-stage epigenetic modification during somatic cell reprogramming by Parp1 and Tet2. *Nature*. 2012;488(7413):652-655.

36. Ficz G, Branco MR, Seisenberger S, et al. Dynamic regulation of 5-hydroxymethylcytosine in mouse ES cells and during differentiation. *Nature*. 2011;473(7347):398-402.

37. Koh KP, Yabuuchi A, Rao S, et al. Tet1 and Tet2 regulate 5-hydroxymethylcytosine production and cell lineage specification in mouse embryonic stem cells. *Cell Stem Cell*. 2011;8(2):200-213.

38. Zhang Q, Zhao K, Shen Q, et al. Tet2 is required to resolve inflammation by recruiting Hdac2 to specifically repress IL-6. *Nature*. 2015;525(7569):389-393.

39. Jaiswal S, Natarajan P, Silver AJ, et al. Clonal Hematopoiesis and Risk of Atherosclerotic Cardiovascular Disease. *N Engl J Med*. 2017;377(2):111-121.

40. Fuster JJ, MacLauchlan S, Zuriaga MA, et al. Clonal hematopoiesis associated with TET2 deficiency accelerates atherosclerosis development in mice. *Science*. 2017;355(6327):842-847.

41. Dawlaty MM, Ganz K, Powell BE, et al. Tet1 is dispensable for maintaining pluripotency and its loss is compatible with embryonic and postnatal development. *Cell Stem Cell*. 2011;9(2):166-175.

42. Liu B, Mink S, Wong KA, et al. PIAS1 selectively inhibits interferon-inducible genes and is important in innate immunity. *Nat Immunol*. 2004;5(9):891-898.

43. Wingett SW, Andrews S. FastQ Screen: A tool for multi-genome mapping and quality control. *F1000Res*. 2018;7:1338.

44. Molder F, Jablonski KP, Letcher B, et al. Sustainable data analysis with Snakemake. *F1000Res*. 2021;10:33.

45. Dobin A, Davis CA, Schlesinger F, et al. STAR: ultrafast universal RNA-seq aligner. *Bioinformatics*. 2013;29(1):15-21.

46. Sun J, Nishiyama T, Shimizu K, Kadota K. TCC: an R package for comparing tag count data with robust normalization strategies. *BMC Bioinformatics*. 2013;14:219.

47. Robinson MD, McCarthy DJ, Smyth GK. edgeR: a Bioconductor package for differential expression analysis of digital gene expression data. *Bioinformatics*. 2010;26(1):139-140.

48. Misharin AV, Morales-Nebreda L, Mutlu GM, Budinger GR, Perlman H. Flow cytometric analysis of macrophages and dendritic cell subsets in the mouse lung. *Am J Respir Cell Mol Biol*. 2013;49(4):503-510.

49. Stevens WW, Kim TS, Pujanauski LM, Hao X, Braciale TJ. Detection and quantitation of eosinophils in the murine respiratory tract by flow cytometry. *J Immunol Methods*. 2007;327(1-2):63-74.

50. Sakry D, Trotter J. The role of the NG2 proteoglycan in OPC and CNS network function. *Brain Res*. 2016;1638(Pt B):161-166.

51. Jones KJ, Korb E, Kundel MA, et al. CPEB1 regulates beta-catenin mRNA translation and cell migration in astrocytes. *Glia*. 2008;56(13):1401-1413.

52. Wang LJ, Cheong ML, Lee YS, Lee MT, Chen H. High-temperature requirement protein A4 (HtrA4) suppresses the fusogenic activity of syncytin-1 and promotes trophoblast invasion. *Mol Cell Biol*. 2012;32(18):3707-3717.

53. Sarkar A, Chanda A, Regmi SC, et al. Recombinant human PRG4 (rhPRG4) suppresses breast cancer cell invasion by inhibiting TGFbeta-Hyaluronan-CD44 signalling pathway. *PLoS One*. 2019;14(7):e0219697.

54. Ho WL, Che MI, Chou CH, et al. B3GNT3 expression suppresses cell migration and invasion and predicts favorable outcomes in neuroblastoma. *Cancer Sci*. 2013;104(12):1600-1608.

55. Veerman K, Tardiveau C, Martins F, Coudert J, Girard JP. Single-Cell Analysis Reveals Heterogeneity of High Endothelial Venules and Different Regulation of Genes Controlling Lymphocyte Entry to Lymph Nodes. *Cell Rep*. 2019;26(11):3116-3131 e3115.

56. Guo JU, Su Y, Zhong C, Ming GL, Song H. Hydroxylation of 5-methylcytosine by TET1 promotes active DNA demethylation in the adult brain. *Cell*. 2011;145(3):423-434.

57. Dhaliwal K, Scholefield E, Ferenbach D, et al. Monocytes control second-phase neutrophil emigration in established lipopolysaccharide-induced murine lung injury. *Am J Respir Crit Care Med*. 2012;186(6):514-524.

58. Kitamura Y, Hashimoto S, Mizuta N, et al. Fas/FasL-dependent apoptosis of alveolar cells after lipopolysaccharide-induced lung injury in mice. *Am J Respir Crit Care Med*. 2001;163(3 Pt 1):762-769.

59. Fujita M, Kuwano K, Kunitake R, et al. Endothelial cell apoptosis in lipopolysaccharide-induced lung injury in mice. *Int Arch Allergy Immunol*. 1998;117(3):202-208.

60. Ogata-Suetsugu S, Yanagihara T, Hamada N, et al. Amphiregulin suppresses epithelial cell apoptosis in lipopolysaccharide-induced lung injury in mice. *Biochem Biophys Res Commun*. 2017;484(2):422-428.

61. Grivennikov SI, Tumanov AV, Liepinsh DJ, et al. Distinct and nonredundant in vivo functions of TNF produced by t cells and macrophages/neutrophils: protective and deleterious effects. *Immunity*. 2005;22(1):93-104.

62. Minn AJ, Gupta GP, Siegel PM, et al. Genes that mediate breast cancer metastasis to lung. *Nature*. 2005;436(7050):518-524.

63. Wang D, Sun H, Wei J, Cen B, DuBois RN. CXCL1 Is Critical for Premetastatic Niche Formation and Metastasis in Colorectal Cancer. *Cancer Res*. 2017;77(13):3655-3665.

64. Schliehe C, Flynn EK, Vilagos B, et al. The methyltransferase Setdb2 mediates virus-induced susceptibility to bacterial superinfection. *Nat Immunol*. 2015;16(1):67-74.

Figure legends

Figure 1. RNA-seq analysis of WT and *Tet1*$^{-/-}$ BMDMs upon LPS stimulation. (A) TET1 is induced by TLR signaling. Quantitative real time polymerase chain reaction (Q-PCR) analysis of *Tet1* expression in WT and *Tet1*$^{-/-}$ BMDMs in response to LPS (10ug/ml), Zymosan (50 ug/ml), Poly (I:C) (20 ug/ml), IFNγ (5 ng/ml), and IL-4 (10 ng/ml) for various time periods as indicated. (B) and (C) Heat maps of the differentially expressed genes (fold change > 2; adjusted P value < 0.05) in untreated WT (WU) vs untreated *Tet1*$^{-/-}$ (KU) BMDMs (B) and WT (WL) vs *Tet1*$^{-/-}$ (KL) BMDMs treated with LPS for 4 hr (C). WU: wild type untreated; KU: knockout untreated; WL: wild type treated with LPS; KL: knockout treated with LPS. WU1-3 and KU1-3 represent independent biological samples.

Figure 2. TET1 selectively regulates the expression of a subset of genes in response to inflammatory stimuli. (A) Q-PCR analysis of gene expression in WT and *Tet1*$^{-/-}$ BMDMs treated with LPS (10 ng/ml) for 2 hr, 6 hr, and 24 hr as indicated. (B) Same as in (A) except RNA samples prepared from primary embryonic fibroblasts (MEFs) treated with TNFα (20 ng/ml) for 30 min or 2 hr or treated with IFNγ (5 ng/ml) for 1hr and 3 hr as indicated. Shown is the representative result from at least 3 independent experiments. Error bars represent SD.

Figure 3. TET1 regulates the DNA methylation of the *Cxcl1* promoter in BMDMs. (A) Diagram of the murine *Cxcl1* promoter region approximately from -700 bp to +500 bp of the transcription start site. Short vertical lines represent potential CpG methylation sites. Regions #1 and #2 indicate two areas of interest for methylation analysis. (B) Methylation analysis of the *Cxcl1* promoter region#1 was performed by bisulfite conversion of genomic DNA from WT and *Tet1*$^{-/-}$ BMDMs. The *x* axis represents the positions of the CpG sites relative to the transcription

start site (+1); the *y* axis represents the percentage. Closed circle: methylated cytosine; Open circle: unmethylated cytosine.

Figure 4. TET1 regulates the DNA methylation of the *Cxcl1* promoter in primary fibroblasts. Methylation analysis of the *Cxcl1* promoter region#1 was performed by bisulfite conversion of genomic DNA from WT and *Tet1*$^{-/-}$ primary embryonic fibroblasts (MEFs) untreated or treated with TNFα (20 ng/ml) for 3 hr as indicated. The *x* axis represents the positions of the CpG sites relative to the transcription start site (+1); the *y* axis represents the percentage. Closed circle: methylated cytosine; Open circle: unmethylated cytosine.

Figure 5. Analysis of the effect of DNA methylation of the *Cxcl1* gene promoter. (A) 293T cells were transfected with the empty vector control (pGL3) or the *Cxcl1* promoter containing plasmid (pCXCL1 promoter). Cells were then untreated with treated with human TNFα (10ng/ml) followed by luciferase assays. (B) Same as in (A) except 293T cells were transfected with the unmethylated *Cxcl1* promoter or the cytosine methylated *Cxcl1* promoter generated by *in vitro* treatments with or without the CpG methyltransferase M.SssI before plasmid ligation as indicated. Shown is the representative result of three independent experiments. Error bars represent SD.

Figure 6. Defective neutrophil recuriment and *Cxcl1* production in BAL fluid of *Tet1*$^{-/-}$ mice in LPS-induced acute lung injury. (A) WT and *Tet1*$^{-/-}$ mice were intranasally injected with LPS (0.5mg/kg) for 4 hr, and Bronchoalveolar lavage (BAL) fluids were collected and analyzed by flow cytometry. Data were analyzed using the FlowJo software. Neutrophils were gated as CD45^{+}CD11b^{+}Ly6G^{+} cells, macrophages were identified as CD45^{+}CD11c^{+}SiglecF^{+} population of cells, and eosinophils were defined as CD45^{+}CD11c$^{low/-}$SiglecF^{+} cells. WT (n=4),

Tet1$^{+/-}$ (n=7), and *Tet1*$^{-/-}$ (n=9). (B) The CXCL1 protein levels in BAL fluids from mice treated with LPS by intranasal injections for 4 hr were measured by ELISA assays. The *Tet1*$^{+/+}$ and *Tet1*$^{+/-}$ group (n=8); *Tet1*$^{-/-}$ (n=6). (C) Same as in (B) except TNFα protein was measured by ELISA assays. The *Tet1*$^{+/+}$ and *Tet1*$^{+/-}$ group (n=5); *Tet1*$^{-/-}$ (n=5). (D) Q-PCR analysis of RNA samples prepared from total cells obtained from the BAL fluid from two independent pairs of WT and *Tet1*$^{-/-}$ mice treated intranasally with PBS or LPS (0.5 mg/kg) for 16 hr. *P* values were determined by non-paired *t*-test.

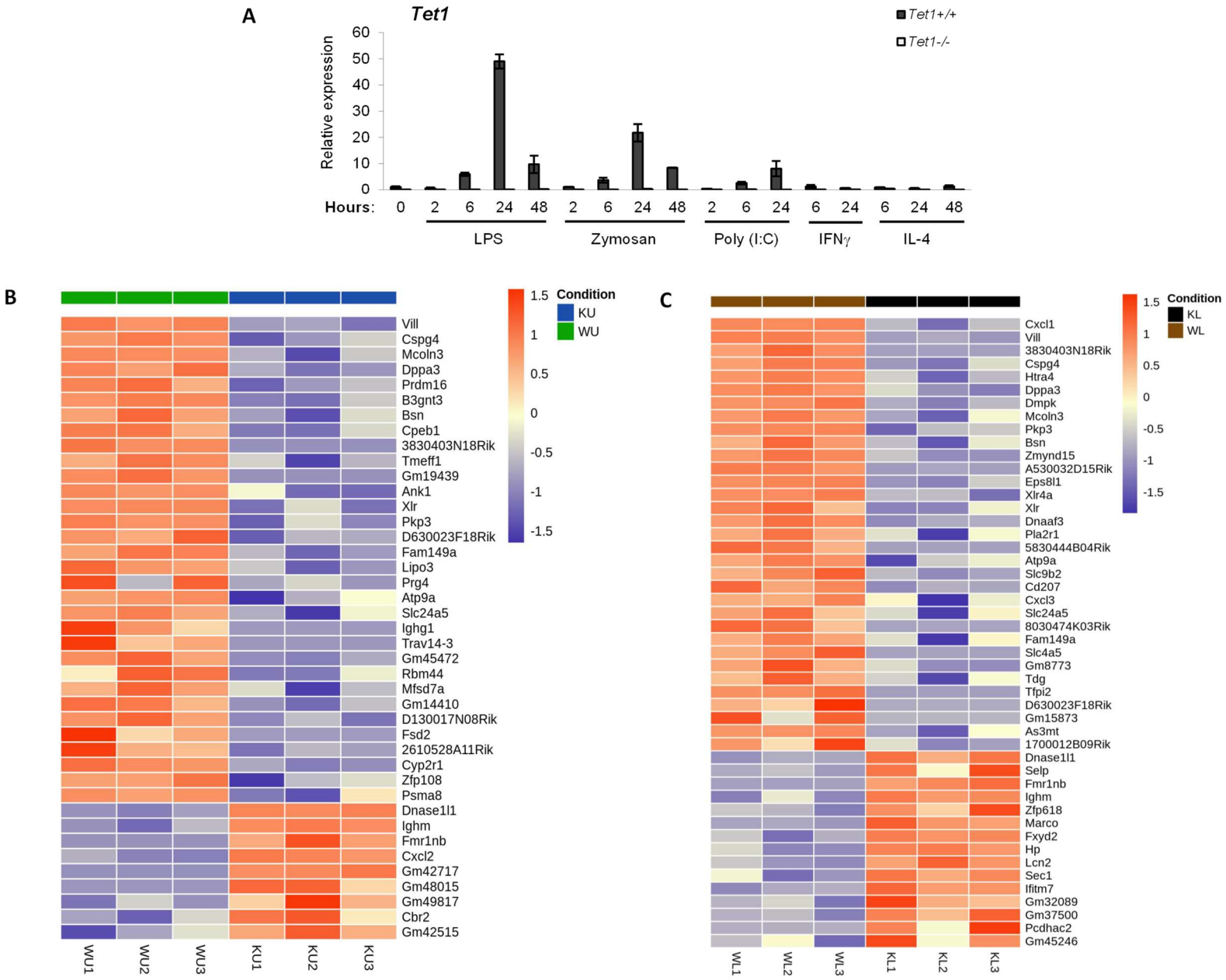
A
Tet1
Tet1+/+
Tet1-/-
Relative expression
60
50
40
30
20
10
0
Hours: 0 2 6 24 48 2 6 24 48 2 6 24 6 24 6 24 48
LPS
Zymosan
Poly (I:C)
IFNγ
IL-4
B
Condition
KU
WU
1.5
1
0.5
0
-0.5
-1
-1.5
Vill
Cspg4
Mcoln3
Dppa3
Prdm16
B3gnt3
Bsn
Cpeb1
3830403N18Rik
Tmeff1
Gm19439
Ank1
Xlr
Pkp3
D630023F18Rik
Fam149a
Lipo3
Prg4
Atp9a
Slc24a5
Ighg1
Trav14-3
Gm45472
Rbm44
Mfsd7a
Gm14410
D130017N08Rik
Fsd2
2610528A11Rik
Cyp2r1
Zfp108
Psma8
Dnase1l1
Ighm
Fmr1nb
Cxcl2
Gm42717
Gm48015
Gm49817
Cbr2
Gm42515
WU1
WU2
WU3
KU1
KU2
KU3
C
Condition
KL
WL
1.5
1
0.5
0
-0.5
-1
-1.5
Cxcl1
Vill
3830403N18Rik
Cspg4
Htra4
Dppa3
Dmpk
Mcoln3
Pkp3
Bsn
Zmynd15
A530032D15Rik
Eps8l1
Xlr4a
Xlr
Dnaaf3
Pla2r1
5830444B04Rik
Atp9a
Slc9b2
Cd207
Cxcl3
Slc24a5
8030474K03Rik
Fam149a
Slc4a5
Gm8773
Tdg
Tfpi2
D630023F18Rik
Gm15873
As3mt
1700012B09Rik
Dnase1l1
Selp
Fmr1nb
Ighm
Zfp618
Marco
Fxyd2
Hp
Lcn2
Sec1
Ifitm7
Gm32089
Gm37500
Pcdhac2
Gm45246
WL1
WL2
WL3
KL1
KL2
KL3

Figure 1

A

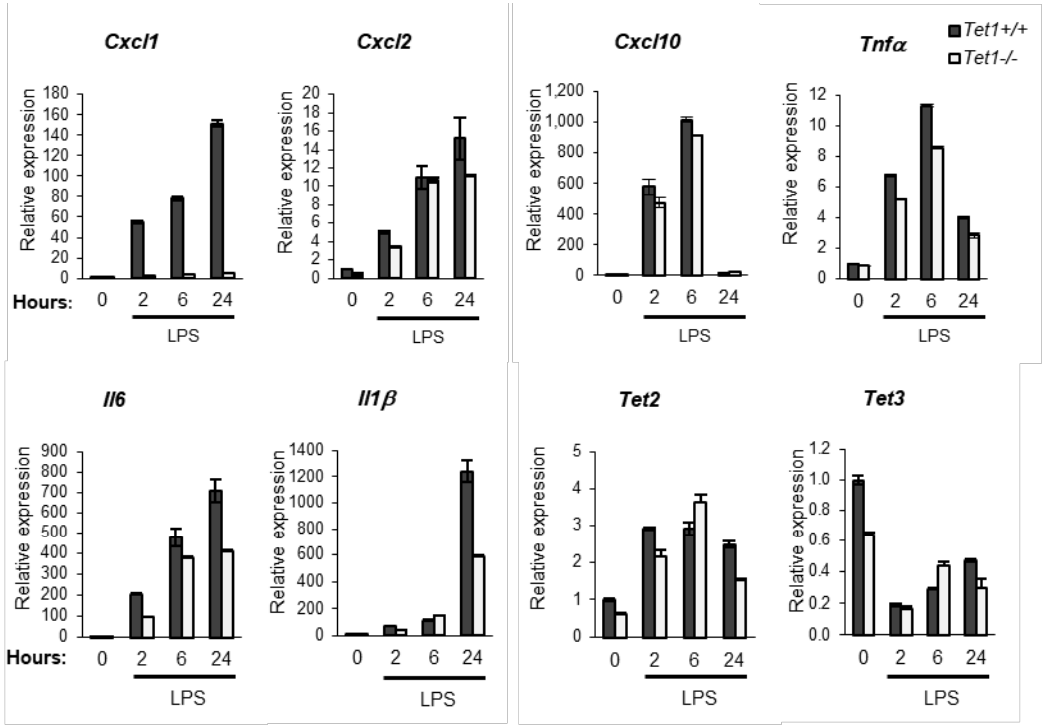
Cxcl1
Cxcl2
Cxcl10
Tnfα
Tet1+/+
Tet1-/-
Il6
Il1β
Tet2
Tet3
Relative expression
Hours:
0 2 6 24
LPS

B

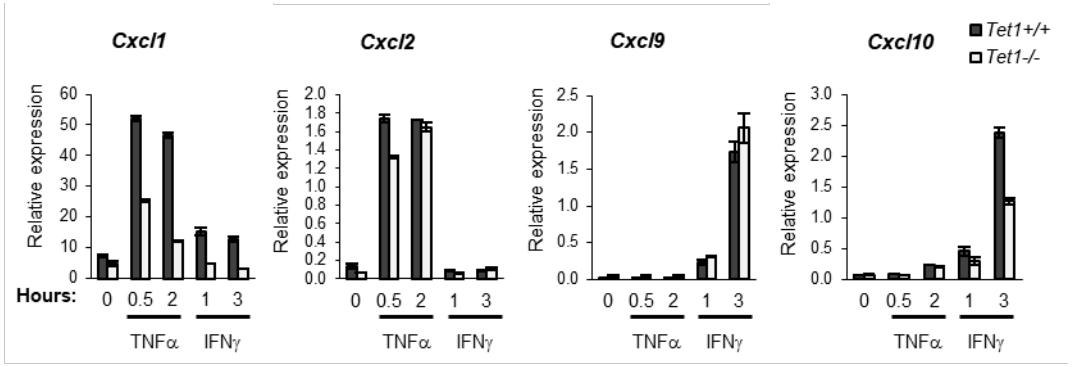
Cxcl1
Cxcl2
Cxcl9
Cxcl10
Tet1+/+
Tet1-/-
Relative expression
Hours:
0 0.5 2 1 3
TNFα IFNγ

Figure 2

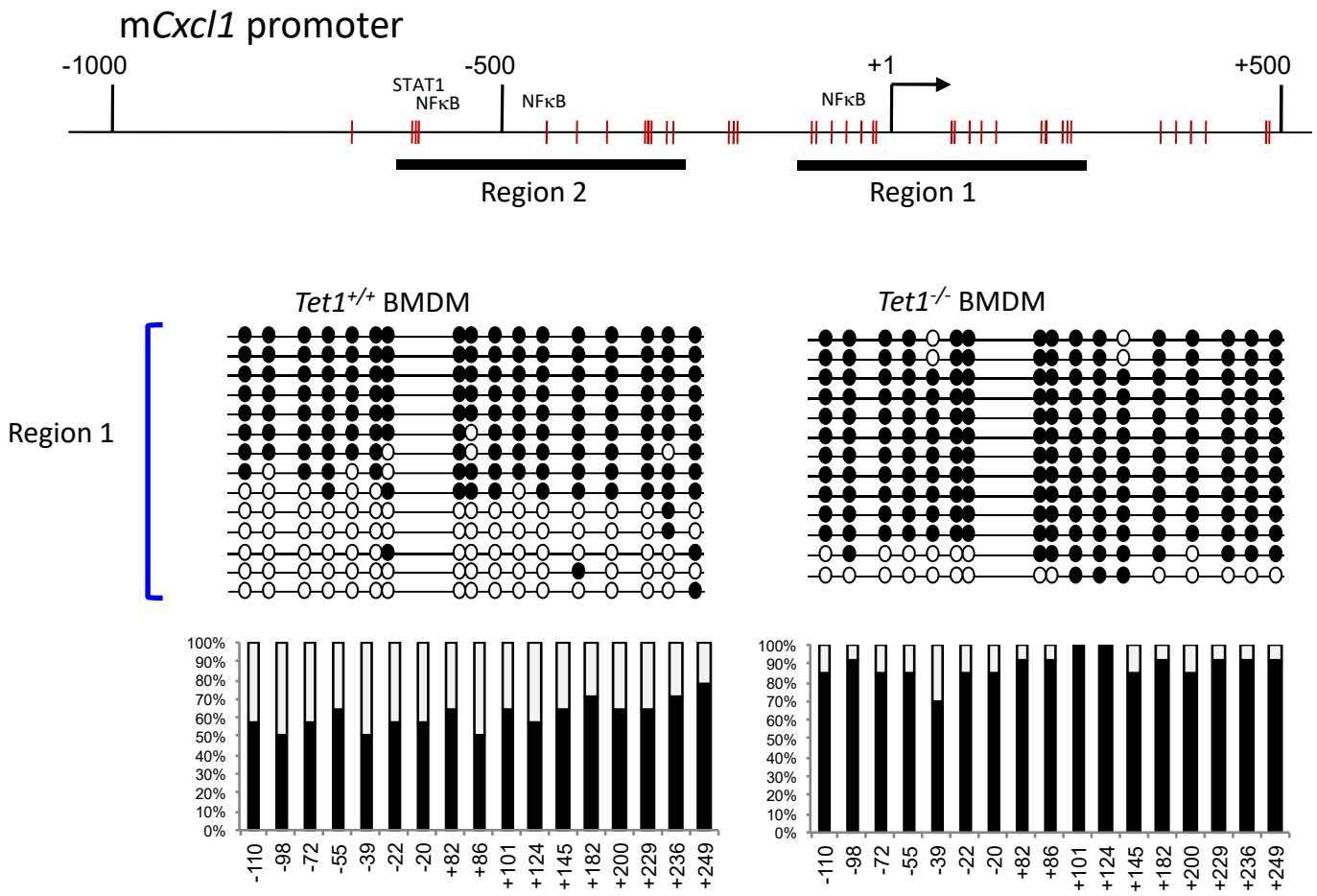
mCxcl1 promoter
-1000
-500
+1
+500
STAT1
NFκB
NFκB
NFκB
Region 2
Region 1
Tet1+/+ BMDM
Tet1-/- BMDM
Region 1
100%
90%
80%
70%
60%
50%
40%
30%
20%
10%
0%
-110
-98
-72
-55
-39
-22
-20
+82
+86
+101
+124
+145
+182
+200
+229
+236
+249

Figure 3

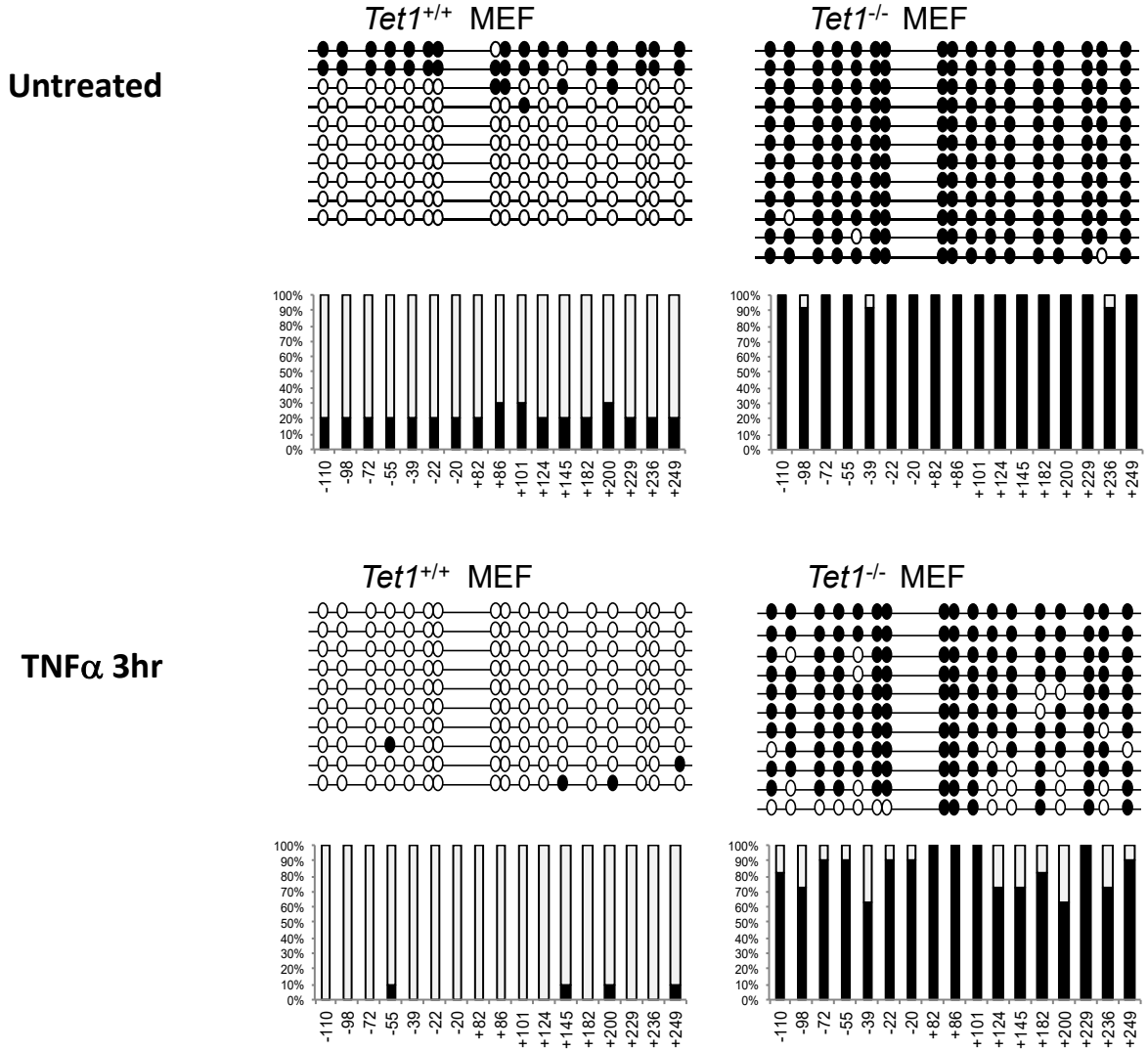
Untreated
Tet1+/+ MEF
Tet1-/- MEF
TNFα 3hr
Tet1+/+ MEF
Tet1-/- MEF
100%
90%
80%
70%
60%
50%
40%
30%
20%
10%
0%
-110
-98
-72
-55
-39
-22
-20
+82
+86
+101
+124
+145
+182
+200
+229
+236
+249

Figure 4

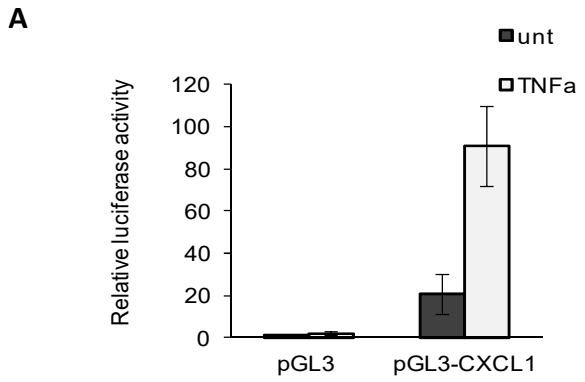
A
unt
TNFa
Relative luciferase activity
120
100
80
60
40
20
0
pGL3
pGL3-CXCL1

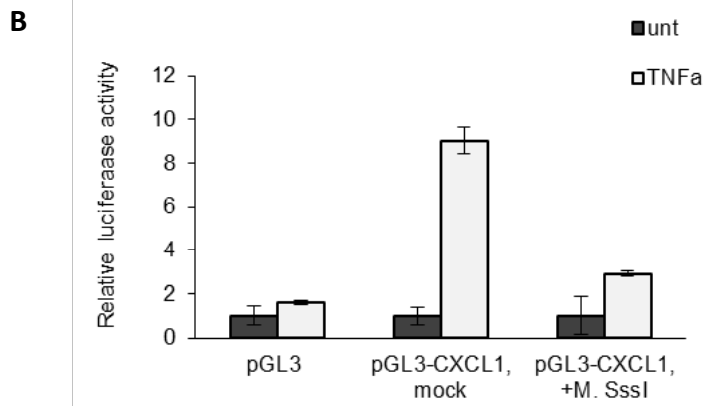
B
unt
TNFa
Relative luciferaase activity
12
10
8
6
4
2
0
pGL3
pGL3-CXCL1, mock
pGL3-CXCL1, +M. SssI

Figure 5

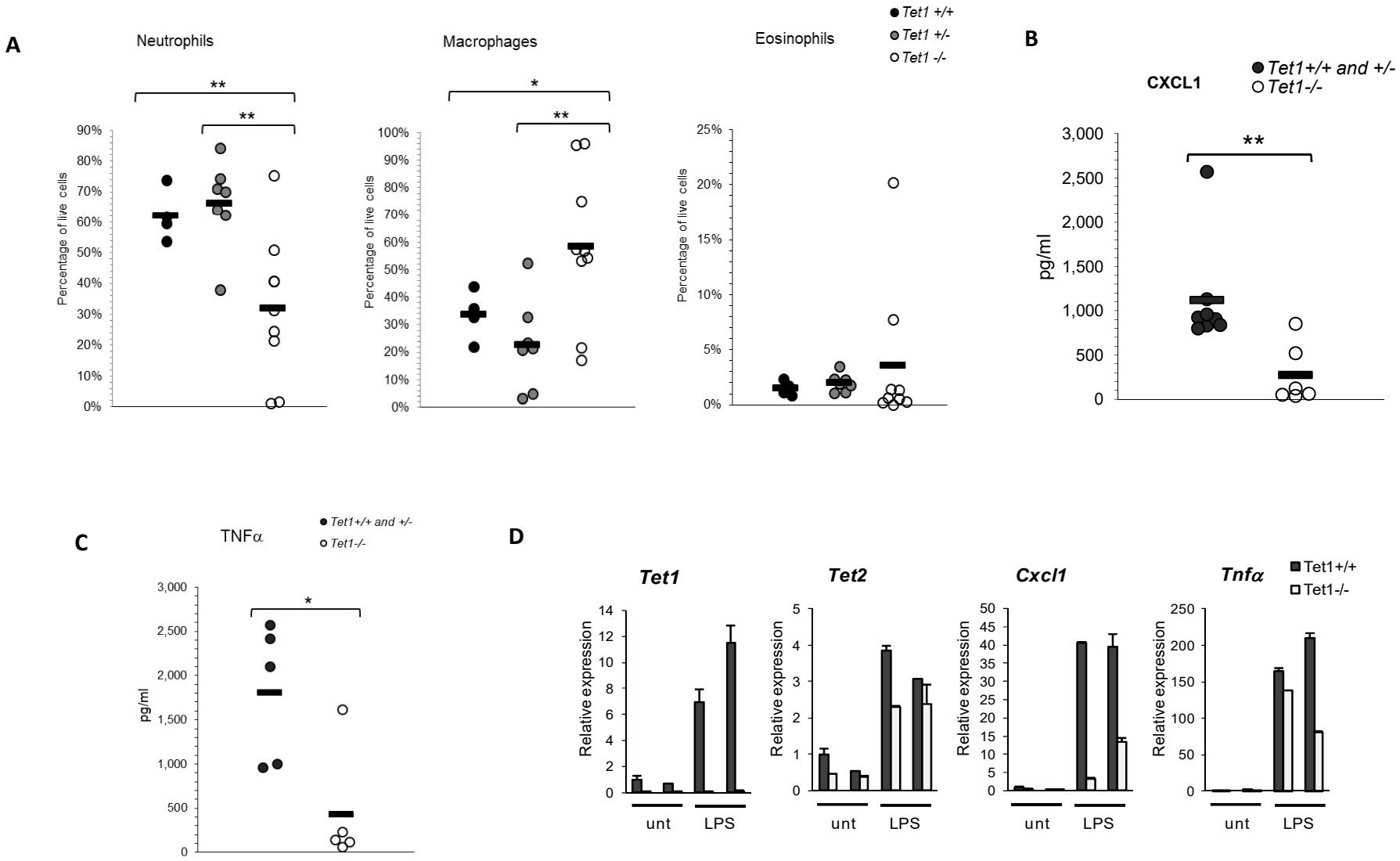
A
Neutrophils
Macrophages
Eosinophils
Tet1 +/+
Tet1 +/-
Tet1 -/-
Percentage of live cells
B
CXCL1
Tet1+/+ and +/-
Tet1-/-
pg/ml
C
TNFα
Tet1+/+ and +/-
Tet1-/-
pg/ml
D
Tet1
Tet2
Cxcl1
Tnfα
Tet1+/+
Tet1-/-
Relative expression
unt
LPS

Figure 6

Supplementary Data

TET1 controls *Cxcl1* induction by DNA demethylation and promotes neutrophil recruitment during acute lung injury

Kathleen M. Yee[1, 2], Richard W. Shuai[3], Bin Liu[1], Christian A. Huynh[1], Chao Niu[1], Hailey R. Lee[1], Min S. Lee[1],Jirui Wen[4, 5], Jian Zou[4, 6*], Jiang Wu[4*], and Ke Shuai[1,2*]

Material and methods

Cell culture

Mouse bone marrow-derived dendritic cells (BMDC): Bone marrow was collected and red blood cells lysed similarly as for BMDM indicated above. Then 2 x10^6 cells were seeded per 35 mm well with 1.5 ml of complete RPMI containing 10% FBS, 1% penicillin-streptomycin and 20 ng/ml recombinant murine GM-CSF (PeproTech). On day 2 and day 4, most of the media was carefully removed to avoid disturbing the non-adherent cells, and replaced with 1.5 ml of fresh, complete RPMI. On day 6, the non-adherent cells were collected and reseeded onto fresh plates. On day 7, cells were used for treatment assays.

Peritoneal macrophages: Peritoneal cell exudate (PEC) was harvested by careful injection of 5 ml of cold serum-free RPMI into the peritoneal cavity of ethanized mice via a 25 G needle and 5 ml syringe. Care was placed to avoid puncturing major organs and blood vessels. The peritoneum was then gently massaged for a few seconds to loosen any attached cells into the RPMI solution. Then using the same needle and syringe, the injected RPMI was carefully collected. The procedure was repeated with another 5 ml of RPMI, for a total volume of 10 ml.

Samples with blood were discarded. PEC was washed once with PBS, then resuspended in complete RPMI containing 10% FBS and 1% penicillin-streptomycin. Cells were seeded onto 12-well plates and placed in a 37°C tissue-culture incubator. The next day, non-adherent cells were washed off with PBS. Fresh complete media was added to the adherent cells (i.e. peritoneal macrophages). After resting cells for at least an hour in the incubator, cells were then used for experiments.

Figure legends

Figure S1. Gene-dosage effect of *Tet1* on Cxcl1 induction in response to LPS in BMDMs. Q-PCR analysis of *Cxcl1* induction in BMDMs prepared from WT [(1)], *Tet1*$^{+/-}$ [(2), (3)], *Tet1*$^{-/-}$ [(4), (5)] treated with LPS (10ng/ml) for 4 hr and 24 hr as indicated. Error bars represent SD.

Figure S2. The effect of TET1 on Cxcl1 induction in peritoneal macrophages and BMDCs. (A) Q-PCR analysis of *Cxcl1* and *Cxcl2* induction in primary peritoneal macrophages of WT and *Tet1*$^{-/-}$ mice untreated or treated with LPS (10ng/ml) for 2 hr. (B) Same as in (A) except RNA samples from BMDCs were used. Error bars represent SD.

Figure S3. Analysis of DNA methylation in the region #2 of the *Cxcl1* promoter in BMDMs. Methylation analysis of the *Cxcl1* promoter region#2 was performed by bisulfite conversion of genomic DNA from WT and *Tet1*$^{-/-}$ BMDMs. The *x* axis represents the positions of the CpG sites relative to the transcription start site (□1); the *y* axis represents the percentage. Closed circle: methylated cytosine; Open circle: unmethylated cytosine.

Figure S4. TET1 regulates the DNA methylation of the *Cxcl1* promoter in peritoneal macrophages. Methylation analysis of the *Cxcl1* promoter region#1 was performed by bisulfite

conversion of genomic DNA from WT and *Tet1*$^{-/-}$ peritoneal macrophages. The *x* axis represents the positions of the CpG sites relative to the transcription start site (□1); the *y* axis represents the percentage. Closed circle: methylated cytosine; Open circle: unmethylated cytosine.

Figure S5. List of Q-PCR primers. See detailed description in the figure.

Figure S6. List of key reagents. See detailed description in the figure.

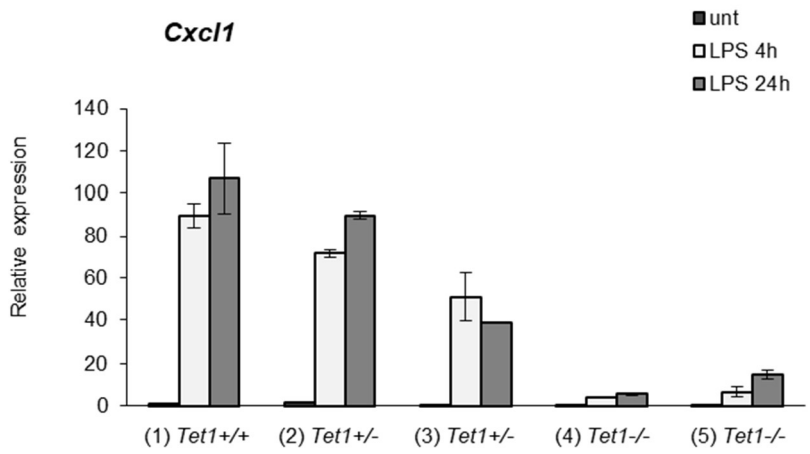
Cxcl1
unt
LPS 4h
LPS 24h
Relative expression
140
120
100
80
60
40
20
0
(1) Tet1+/+
(2) Tet1+/-
(3) Tet1+/-
(4) Tet1-/-
(5) Tet1-/-

Figure S1

A

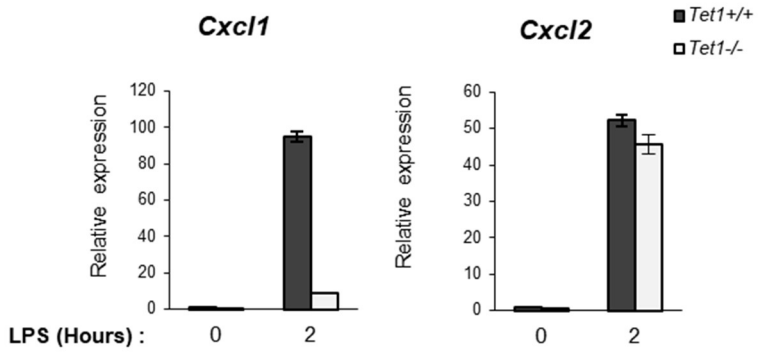
Cxcl1
Cxcl2
Tet1+/+
Tet1-/-
Relative expression
LPS (Hours) :
0
2

B

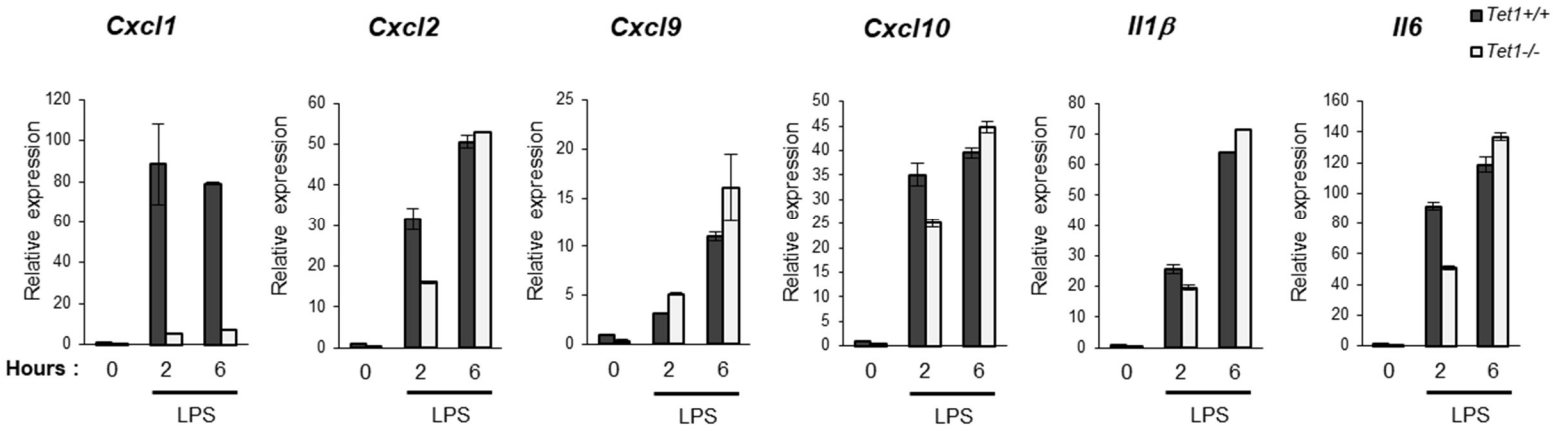
Cxcl1
Cxcl2
Cxcl9
Cxcl10
Il1β
Il6
Tet1+/+
Tet1-/-
Relative expression
Hours :
0
2
6
LPS

Figure S2

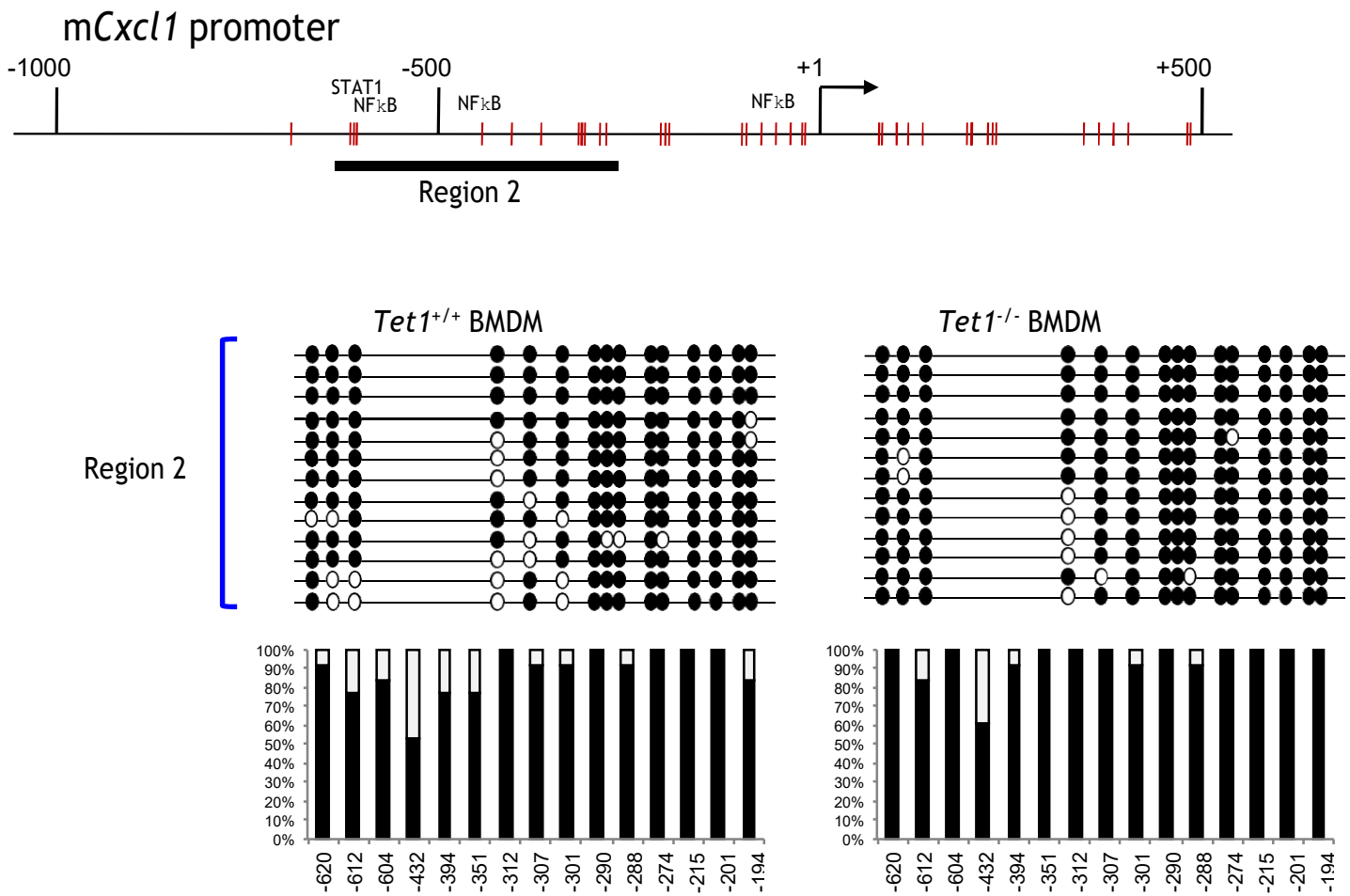
mCxcl1 promoter
-1000
-500
+1
+500
STAT1
NFkB
NFkB
NFkB
Region 2
Tet1+/+ BMDM
Tet1-/- BMDM
Region 2
100%
90%
80%
70%
60%
50%
40%
30%
20%
10%
0%
-620
-612
-604
-432
-394
-351
-312
-307
-301
-290
-288
-274
-215
-201
-194

Figure S3

CpG Methylation Analysis

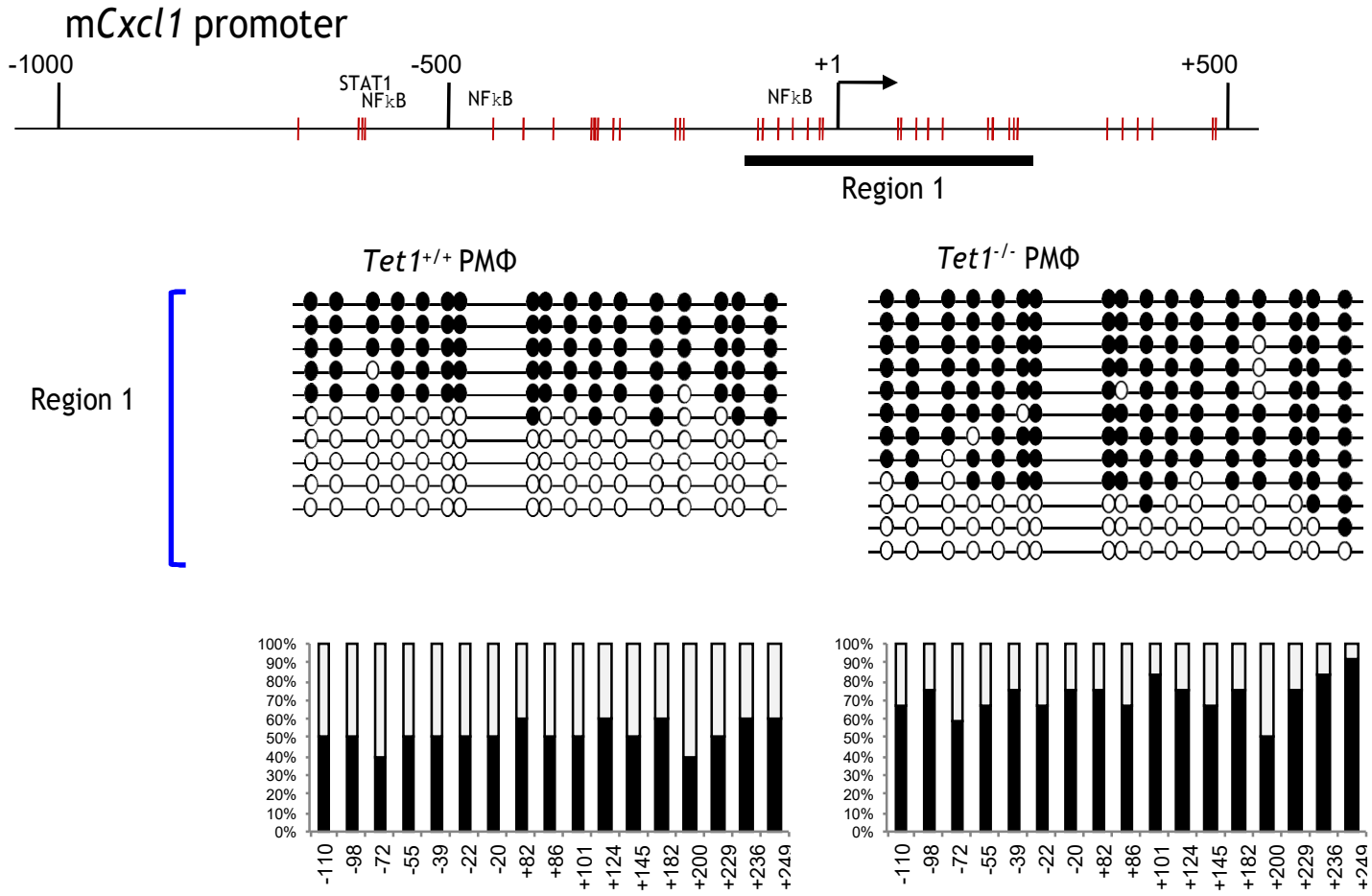

Figure S4

Q-PCR primers	
Hprt	5'-CAGTACAGCCCCAAAATGGT
	3'-CAAGGGCATATCCAACAACA
Gapdh	5'-AACTTTGGCATTGTGGAAGG
	3'-GGATGCAGGGATGATGTTCT
Tet1	5'-CTGCACCCTGTGACTGTGAT
	3'-GTCTCCATGAGCTCCCTGAC
Tet2	5'-TGATCCAGGAGGAGCAGTGA
	3'-CGGGCTTCCATTCTGGAGTT
Tet3	5'-TCCGGATTGAGAAGGTCATC
	3'-CCAGGCCAGGATCAAGATAA
Cxcl1	5'-GTCAGTGCCTGCAGACCAT
	3'-CGACCATTCTTGAGTGTGGC
Cxcl2	5'-ATCCAGAGCTTGAGTGTGACGC
	3'-AAGGCAAACTTTTTGACCGCC
Cxcl9	5'-CTTTTCCTTTTGGGCATCATCT
	3'-GCAGGAGCATCGTGCATTC
Cxcl10	5'-CCTGCCCACGTGTTGAGAT
	3'-TGATGGTCTTAGATTCCGGATTC
Tnfa	5'-CAGACCCTCACACTCAGATCA
	3'-ACAAGGTACAACCCATCGGC
Il-6	5'-CACTTCACAAGTCGGAGGCT
	3'-CTGCAAGTGCATCATCGTTGT
Il-1b	5'-AGCTTCCTTGTGCAAGTGTCT
	3'-GACAGCCCAGGTCAAAGGTT

Figure S5

List of key reagents					
Antibody Name		**Antibody Clone**	**Company**		Catalog #
PE/Dazzle™ 594 anti-mouse/human CD11b Antibody		M1/70	Biolegend		101256
PE/Cy7 anti-mouse CD45 Antibody		30-F11	Biolegend		103113
APC anti-mouse CD11c Antibody		N418	Biolegend		117309
PerCP/Cy5.5 anti-mouse Ly-6G Antibody		1A8	Biolegend		127615
PE Rat Anti-Mouse Siglec-F		E50-2440	BD Pharmingen		562068
Cytokines	**Company**				
m TNFa	PeproTech				
h TNFa	PeproTech				
m IFNg	PeproTech				
m IL4	PeproTech				
HMW Poly (I:C)	Sigma				
LPS	Sigma				
Zymosan	Sigma				

Figure S6